In Situ Observation of the Thermochromic Phase Transition of the Merocyanine J-Aggregates Monolayer at the Air−Water Interface Using External Infrared Reflection Absorption Spectroscopy

Noritaka Kato,*,† Masato Yamamoto,‡ Koichi Itoh,§ and Yoshiaki Uesu†

Department of Physics, Waseda University, 3-4-1, Okubo, Shinjuku-ku, 169-8555 Tokyo, Japan, Department of Chemistry, College of Arts and Sciences, Showa University, 1-5-8, Hatanodai, Shinagawa-ku, 142-8555 Tokyo, Japan, and Department of Chemistry, Waseda University, 3-4-1, Okubo, Shinjuku-ku, 169-8555 Tokyo, Japan

Received: April 21, 2003; In Final Form: August 25, 2003

To understand the mechanism of thermochromic phase transition of a J-aggregate monolayer of a merocyanine dye (MD, 3-caboxymethyl-5-[2-(3-octadecyl-benzothiazolin-2-ylidene)ethylidene]rhodanine) on aqueous subphases containing Mg^{2+} and Cd^{2+} ions, the molecular vibrational investigation was performed by using external infrared (IR) reflection absorption spectroscopy. The in situ observation indicates that, on increasing the subphase temperature from 19.5 to 34.5 °C, IR bands observed at 1177 and 1126 cm^{-1} for the J-aggregate monolayer shift to 1188 and 1146 cm^{-1}, respectively; the shift is reversible and exhibits a thermal-hysteresis. These spectral changes correspond well to the thermochromic behavior of the visible absorption band of the J-aggregate (J-band), where the J-band shift is observed between 620 and 595 nm. The ab initio calculation of the normal modes were carried out on the MD molecule to assign the IR bands near 1183 and 1136 cm^{-1}, indicating that they are attributed by the vibrational modes of the carboxymethyl group coupled with the modes of the thioketon group of the rhodanine ring, the conjugated backbone of the dye, and the benzothiazole group. Both spectroscopic and computational results suggest that the transition from the phase of the J-band at 620 nm to that of the J-band at 595 nm is characterized by the exchange of the metal ion from Mg^{2+} to Cd^{2+} interacting with the MD molecule through the carboxylate group of the carboxymethyl group, and the exchange of metal ion induces the shift of the IR bands as well as the J-band.

Introduction

J-aggregates of cyanine dye molecules have attracted much attention because of their optoelectronic and nonlinear optical properties, such as a model system for electron and energy transfers, a spontaneous response to the laser pulse, and a huge nonlinear susceptibility.[1] It is well-known that J-aggregates are indispensable for the photographic technology using silver halides as spectral sensitizers,[2] and recently, it was reported that J-aggregates are also the candidates for a dye-sensitized solar cell[3] and an all-optical demultiplexer for femtosecond optical pulses.[4] J-aggregates are characterized by the following facts: (i) a sharp visible absorption band (J-band) locates at the lower energy than that of isolated (monomer) dye molecules, (ii) a fluorescence band shows a negligible Stokes shift, and (iii) the aggregate has a highly ordered structure of organic dye molecules.[1] Since the discovery of the J-aggregates,[5,6] many attempts have been performed to establish assembling methods of J-aggregates, to understand their structure and formation mechanism, and to investigate their optical property in various systems in solutions,[7] in vesicles,[8] at interfaces,[9] in layered films,[10] in polymer and silica matrixes,[11] on colloidal particles,[12] in capsules,[13] and on DNA templates.[14]

One of the most interesting issues of the J-aggregates is the development of methods that control the formation of J-aggregates, e.g., the thermal and chemical treatments[15] and the ultra-violet light illumination,[16] which dissociate and restore the J-aggregate state, and the application of magnetic field,[17] which aligns the orientation of J-aggregate assembly. The development of the controlling method is important not only for a practical application such as an optical memory device but also for understanding the aggregation mechanism of dye molecules. Recently, we have found a reversible thermochromic phase transition of J-aggregates formed by amphiphilic merocyanine dye molecules (MD, 3-caboxymethyl-5-[2-(3-octadecyl-benzothiazolin-2-ylidene)ethylidene]rhodanine, see Figure 1a) at the air−water interface.[18,19] Although the monomeric state of the MD molecule gives an absorption band at ca. 525 nm, the J-aggregate on an aqueous subphase containing Cd^{2+} as a counterion exhibits a J-band at ca. 595 nm, and the J-aggregate on an aqueous subphase containing Mg^{2+} exhibits the J-band at ca. 620 nm. When the subphase contains both Cd^{2+} and Mg^{2+}, the reversible thermochromic phase transition takes place, giving the J-band at 595 nm for a high temperature (HT) phase and the band at 620 nm for a low temperature (LT) phase. The J-bands shift discretely at a phase transition temperature, and a thermal-hysteresis is observed for the shift. The transition temperature depends on the molar fraction of $CdCl_2$ and $MgCl_2$ salts ($\rho = [CdCl_2]/([CdCl_2]+[MgCl_2])$) in the subphase, and this behavior is summarized as a (ρ, T) phase diagram in Figure 1b, and the thermal-hysteresis of $\rho = 20\%$ is shown in Figure

* To whom all correspondence should be addressed. E-mail: nkato@kurenai.waseda.jp. Present mailing address (until January 2004): Department of Chemical and Biomolecular Engineering, The University of Melbourne, Victoria 3010, Australia. Phone: +61 3 8344 9833. Fax: +61 3 8344 4153.
† Department of Physics, Waseda University.
‡ Showa University.
§ Department of Chemistry, Waseda University.

10.1021/jp0350621 CCC: $25.00
Published on Web 10/08/2003

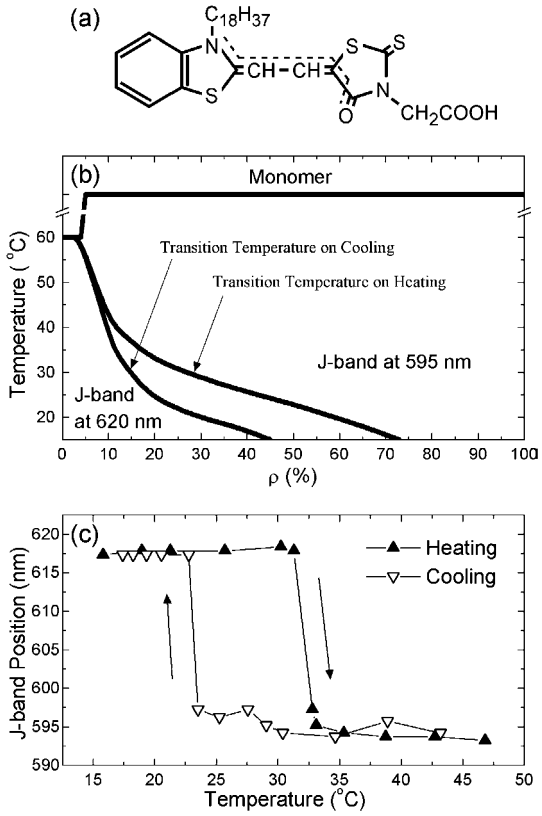

Figure 1. (a) Molecular structure of MD molecule. The dotted line indicates the part of the central conjugated system of the dye. (b) (ρ, T) phase diagram of thermochromic phase transition. (c) Thermal-hysteresis loop of the J-band position obtained at $\rho = 20\%$.

1c. MD molecules immediately form J-aggregates after being spread on these subphases without any compression, and the surface pressure−area isotherm of the MD J-aggregate monolayer does not show any plateau[20] that is typically observed in the extended monolayer as a phase coexistence of two different phases such as liquid-condensed and liquid-expanded phases. Therefore, the MD J-aggregate monolayer is the condensed monolayer,[21] where molecules form crystallites even at extremely low surface pressure, and the reversible thermochromism of J-aggregates is a phase transition of MD crystallites. The in situ observation of the thermochromic phase transition using nonlinear optical microscope revealed that domains of the LT phase grow large in the HT phase matrix on cooling,[18−22] and grazing X-ray diffraction measurements of Langmuir−Blodgett and Langmuir films consisting of the LT or the HT phase suggested that they have different molecular packing structures.[23] These results indicated that this thermochromism is the first-order structural phase transition of two-dimensional crystallites (J-aggregates of MD molecules). We predicted that the chromic phase transition is induced by the mutual recombination of the different counterions to MD molecules; that is, in the LT phase (J-band at 620 nm), MD molecules interact with Mg^{2+} ions, whereas in the HT phase (J-band at 595 nm), they interact with Cd^{2+} ions.[18,19] However, the mechanism of this phase transition has not been fully understood yet.

This work is directed to investigate this thermochromic behavior in terms of molecular vibration of the MD molecule in order to find out their conformational difference between the HT and LT phases. Although many infrared (IR) spectral studies have been carried out on the MD molecule and its derivatives,[15b,24−29] this is the first observation of the MD J-aggregate monolayers at the air−water interface. The in situ observations using external IR reflection absorption spectroscopy[30] were performed on MD J-aggregate monolayers at the air−water interface by changing the subphase temperature. The reversible shift of two IR bands was found. Because ab initio calculations have been shown as a powerful tool for molecular vibrational analyses,[31] the vibrational modes of the shifted bands were clarified by the ab initio calculation based on density functional theory (DFT). The mechanism of the phase transition was discussed based on the clarified vibrational modes of the IR bands.

Experimental Section

Materials. MD molecules were purchased from Hayashibara Biochemical Laboratories, Inc., and their chloroform solution of 1 mmol/L was prepared for the spreading solution. Pure water for the aqueous subphase was made by Puric-Z (ORGANO Co.), and its resistance was greater than 16 MΩ. Three kinds of subphases were used in the present experiments: (i) 0.5 mmol/L $CdCl_2$ ($\rho = 100\%$), (ii) 0.5 mmol/L $MgCl_2$ ($\rho = 0\%$), and (iii) 0.1 mmol/L $CdCl_2$ and 0.4 mmol/L $MgCl_2$ ($\rho = 20\%$). Hereafter, the subphases are abbreviated to subphase[ρ], where $\rho = 0$, 20, and 100%. Every subphases contained ca. 0.05 mmol/L $NaHCO_3$ to stabilize their pH value around at 6.8.

External Infrared Reflection Absorption Spectroscopy. The method of measurement was virtually identical with that already reported.[32] Briefly, a Bio-Rad FTS-45A Fourier transform IR spectrometer with a modified reflection attachment and an MCT detector was used. A Teflon trough was equipped in the sample chamber of the reflection attachment, and the chamber can be purged with dry nitrogen gas. Before spreading MD molecules, the IR spectrum of the air−water interface was taken as a background, and the water vapor component in the IR spectrum was subtracted from the spectrum of the MD J-aggregate monolayer using this background spectrum. To obtain the spectra with good signal-to-noise (S/N) ratio, the humidity in the chamber should be kept constant by adjusting the gas flow with a valve. The measurements were performed at a resolution of 8 cm^{-1} for the monolayer at the interface, and one spectrum was accumulated at least 2048 times. The incident angle of the IR beam was fixed at 30° from the normal direction of the interface. In addition, a transparent IR spectrum of powder MD molecules in a KBr disk was measured with the resolution of 2 cm^{-1} and the accumulation of 1024 times.

Trough and Monolayer Preparation. A rubber heater was placed under the Teflon trough, and its temperature was controlled by a thermal regulator (KP1000, CHINO Corp.). The subphase temperature was monitored by a thermocouple. For the in situ observation, the subphase temperature was varied in a stepwise manner, and the background spectrum at each temperature was measured prior to the measurements of the monolayer. MD molecules form a condensed monolayer and become J-aggregates just after spreading them on the subphase,[19] which means that we do not need to compress the monolayer for inducing the formation of the J-aggregates. Therefore, MD molecules were spread until they filled up the whole surface area of the trough, and the spectrum was measured. The surface pressure was estimated to be smaller than 0.5 mN/m.

Computer Calculations. To make vibrational analyses, an ab initio calculation package of Gaussian 98W[33] was used. The structural optimization and the calculations of vibrational frequencies and modes of the optimized structures were performed by using the DFT method with the functional of BLYP and the 6-31G** basis set.

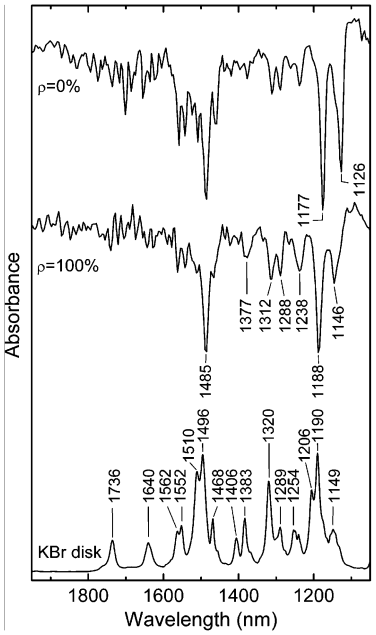

Figure 2. IR spectra of the MD monolayer on subphase[0%] (top) and subphase[100%] (middle) together with that of MD molecules in KBr disk (bottom).

Results and Discussion

IR Spectra of J-Aggregates on Subphase[100%] and Subphase[0%] and MD Molecules in KBr Disk. Figure 2 exhibits the IR spectra of the MD J-aggregate monolayer on subphase[100%], that on subphase[0%], and the transmission IR spectrum of MD molecules dispersed in the KBr disk. The subphase temperature was kept at ca. 20 °C, and the monolayers on subphase[100%] and subphase[0%] exhibit the J-band at 592 and 618 nm, respectively. The IR spectrum of the KBr disk, which corresponds to a non J-aggregate (monomeric) state, agrees with the results of the previous measurements.[15b,25,29] According to their assignments, the vibrational modes of the carboxymethyl and keto groups of the rhodanine ring are observed at 1736 and 1640 cm^{-1}, respectively. The ν_{19}-like modes of phenyl groups are observed at 1468 cm^{-1}, and the central conjugated system of the dye (O═C−C═C−C═C−N, see Figure 1a) contributes to the bands at 1562, 1552, 1510, 1496, 1383, and 1190 cm^{-1}.

There are several differences between the spectrum of the MD molecule in the KBr disk and the MD J-aggregate monolayer on subphase[100%]. First, although the S/N ratios in the 1800∼1600 cm^{-1} region are not high due to the difficulty in the complete subtraction of the water vapor absorption from the spectrum, it is clear that the absorption bands due to the carboxymethyl and keto groups are not discernible in the spectrum, indicating the chelation between the cationic counterion and the carboxylate and keto groups.[15b] Second, several absorption bands of the J-aggregate monolayer on subphase[100%] exhibit the following red-shifts compared to the spectrum of the KBr disk sample; obvious shifts are 1496 → 1485 cm^{-1}, 1383 → 1377 cm^{-1}, and 1320 → 1312 cm^{-1}. These red-shifts have been ascribed to an intramolecular charge transfer caused by the formation of the J-aggregate and/or the coordination interaction between the counterion and the MD molecule; the transfer accompanies a change in the electron configuration of the MD backbone schematically shown by O═C−C═C−C═C−N → $O^{\delta-}$−C−C−C−C−C−$N^{\delta+}$.[15b,25b,27−29] Similar spectral changes have been observed for the Langmuir−Blodgett films of MD molecules in the J-aggregate state by using the IR reflection absorption spectroscopy.[25b]

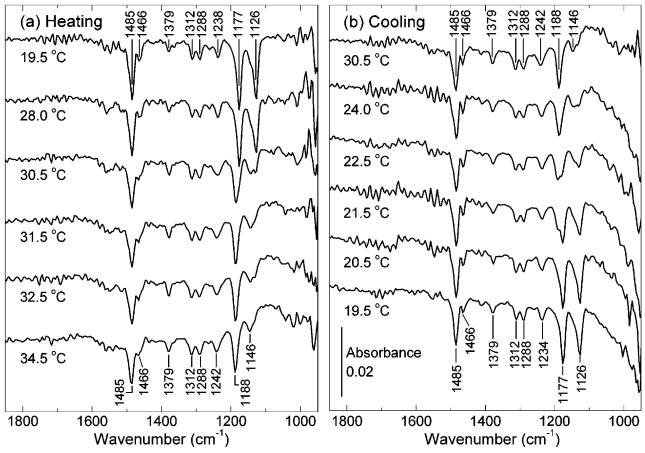

Figure 3. In situ observation of the MD monolayer on subphase[20%] (a) on heating and (b) on cooling.

Comparison of the IR spectrum of the monolayer on subphase[100%] with that on subphase[0%] indicates that the bands at 1188 and 1146 cm^{-1} observed for the monolayer on subphase[100%] shift to 1177 and 1126 cm^{-1}, respectively, for the monolayer on subphase[0%]. The other bands do not show any frequency change on conversion from subphase[100%] to subphase[0%]. Therefore, the bands at 1177 and 1126 cm^{-1} of the monolayer on subphase[0%] and those at 1188 and 1146 cm^{-1} of the monolayer on subphase[100%] are the marker bands of the MD J-aggregate induced by Mg^{2+} ions and those induced by Cd^{2+} ions, respectively. In other words, the transition between the LT and HT phases can be monitored by observing the frequency shifts between the set of the 1177 and 1126 cm^{-1} bands and that of the 1188 and 1146 cm^{-1} bands.

In Situ Observation of the Phase Transition. Figure 3, parts a and b, illustrates the spectral changes observed for the MD J-aggregate monolayer on subphase[20%] during heating and cooling processes, respectively. The spectrum measured at 19.5 °C in Figure 3a is almost identical with that of the monolayer on subphase[0%] in Figure 2, giving the IR bands at 1177 and 1126 cm^{-1}. Both of the samples give the J-band at 620 nm. Thus, the J-aggregate on subphase[20%] at 19.5 °C and that on subphase[0%] take on an identical molecular conformation having a coordination interaction with the Mg^{2+} counterion.

Upon increasing the temperature, both of the IR bands show a doublet feature, exhibiting a higher frequency component at 30.5 °C (Figure 3a), and finally, the bands are completely replaced by the bands at 1188 and 1146 cm^{-1} at 31.5 °C (Figure 3a). The final spectrum, which does not change on further increase of the temperature up to 34.5 °C, is identical to that of the monolayer on subphase[100%] (Figure 2) within the experimental error. These results indicate that at 31.5 °C the conformation of the MD molecule on subphase[20%] is converted to that of the MD molecule on subphase[100%] and the Mg^{2+} ion is replaced by the Cd^{2+} ion at the coordination site. Thus, the frequency change of the bands corresponds to the phase transition from the LT phase giving the J-band at 620 nm to the HT phase giving the band at 595 nm.

When the subphase temperature is cooled to 30.5 °C, the IR spectrum of the J-aggregate monolayer keeps the feature observed at 34.5 °C. As shown in Figure 3b, on further decrease of the temperature, the bands at 1177 and 1126 cm^{-1} begin to appear at 22.5 °C. By 20.5 °C, the bands at 1188 and 1146 cm^{-1} were apparently replaced by the 1177 and 1126 cm^{-1}

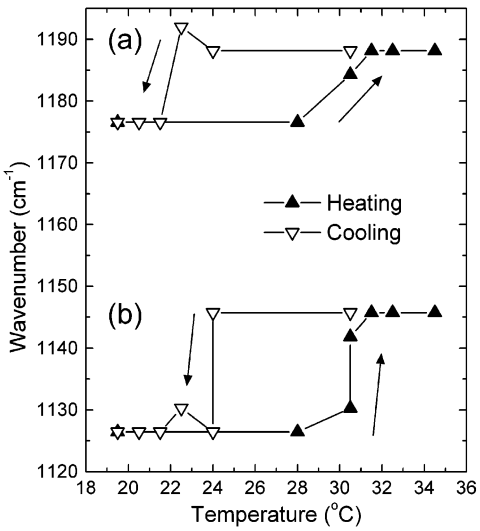

Figure 4. Temperature dependence of the wavenumber of IR bands observed in Figure 3.

bands. Again, the frequency shifts observed for the bands correspond to the transition from the HT phase (J-band at 595 nm) to the LT phase (J-band at 620 nm). The frequency shifts during the heating and cooling processes are summarized in Figure 4, parts a and b. Comparing the results with Figure 1c, we notice the clear parallelism between the thermal-hysteresis of the J-band position and that of the vibrational frequencies. Thus, the driving force of the chromic phase transition of the J-aggregate on the aqueous subphase is the mutual exchange of the Mg^{2+} and Cd^{2+} counterions at coordination sites of the MD molecule; the exchange induces a local conformation change near the coordination sites. The conformation change may induce changes in the degree of intramolecular charge transfer and/or the mode of molecular packing in the J-aggregate,[23] resulting in the change of the J-band position.

Ab Initio Calculation of Molecular Structure. One of the optimized structures of the MD molecule is shown in Figure 5. It has been suggested that the C2−C3═C4−C5, C3═C4−C5═C6, and C4−C5═C6−N7 parts of the MD backbone (see Figure 5a) take a trans conformation.[25,26,34] Based on this conformation of the MD backbone, we adopted two kinds of initial structures for the optimization; that is, one takes a conformation of the C6−N7−C8−C9 dihedral angle of 270°, in which the carboxymethyl group and the octadecyl chain point to the opposite side of the dye backbone, and the other takes the angle of 90°, in which the carboxymethyl group and the octadecyl chain point to the same side of the backbone. The calculation indicated that the optimized structure from the former conformation gives a much lower molecular energy and more planar structure of the dye group compared to that optimized from the latter conformation. The overall structure giving lower energy is shown in Figure 5b, and the optimized value of the dihedral angles of C6−N7−C8−C9 and C12−C11−N10−C2 are 272.97° and 94.04°, respectively. In Table 1, the optimized structural parameters of the chromophore part (O1═C2−C3═C4−C5═C6−N7) of the MD molecule are compared with those determined by X-ray diffraction for a dye molecule in the J-aggregate state.[34] This dye molecule has an identical molecular backbone to that of the MD molecule and includes an ethyl group in the place of octadecyl substituent. The optimization was performed on the MD molecule in the isolated state, and the calculated bond distances and angles show reasonable values (Table 1). The chromophore part of this isolated state exhibits the resonant structure of the π-electron system of the dye

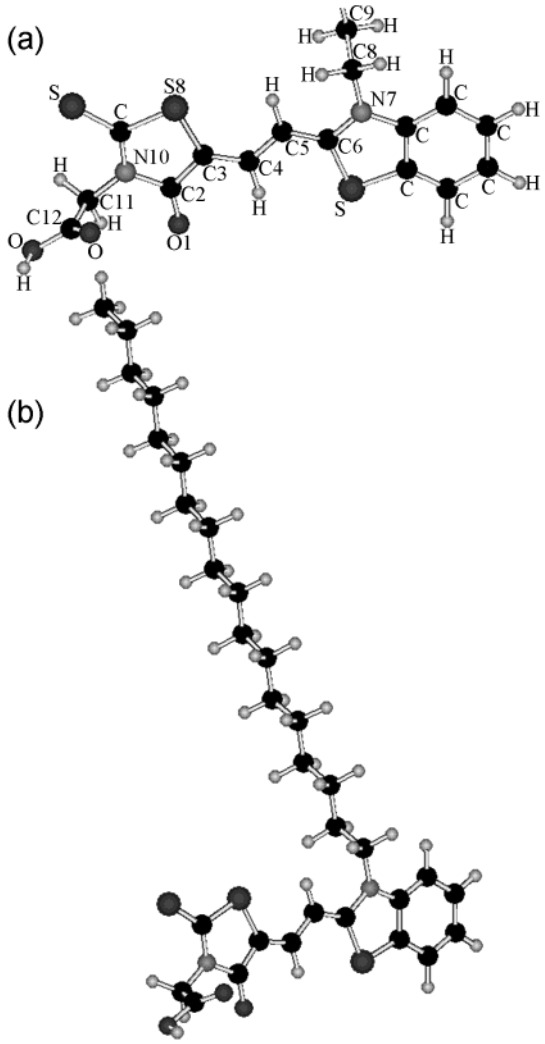

Figure 5. Optimized molecular structure of the MD molecule. (a) Chromophore part and (b) overall structure.

TABLE 1: Bond Distances (Angstroms) and Angles (Degrees) of the Chromophore Obtained from the ab Initio Calculation (Figure 5) and the X-ray Diffraction Analysis of the Crystal

	calculation	crystal[34]
O1−C2	1.236	1.235
C2−C3	1.467	1.428
C3−C4	1.380	1.361
C4−C5	1.420	1.385
C5−C6	1.389	1.375
C6−N7	1.394	1.358
O1−C2−C3	128.1	127.1
C2−C3−C4	122.3	125.0
C3−C4−C5	126.9	125.5
C4−C5−C6	124.4	123.5
C5−C6−N7	125.9	125.0

backbone between O═C−C═C−C═C−N and $O^{\delta-}$−C−C−C−C−C−$N^{\delta+}$.[26b] On the other hand, in the J-aggregate state, the structure of the chromophore part is in the intramolecular charge transfer, i.e., $O^{\delta-}$−C−C−C−C−C−$N^{\delta+}$.[27−29,34] When we normalize the bond length of C2−C3, C3−C4, C4−C5 and C5−C6 by that of C3−C4, the ratio of C2−C3:C3−C4:C4−C5:C5−C6 in the structure of O═C−C═C−C═C−N is 1.15:1:1.15:1, which is derived by using the typical value of the C−C single bond (1.54 Å) and that of the C═C bond length (1.34 Å) for simplicity. When this ratio is calculated by using the values of the J-aggregates crystal[34] (Table 1), the ratio becomes

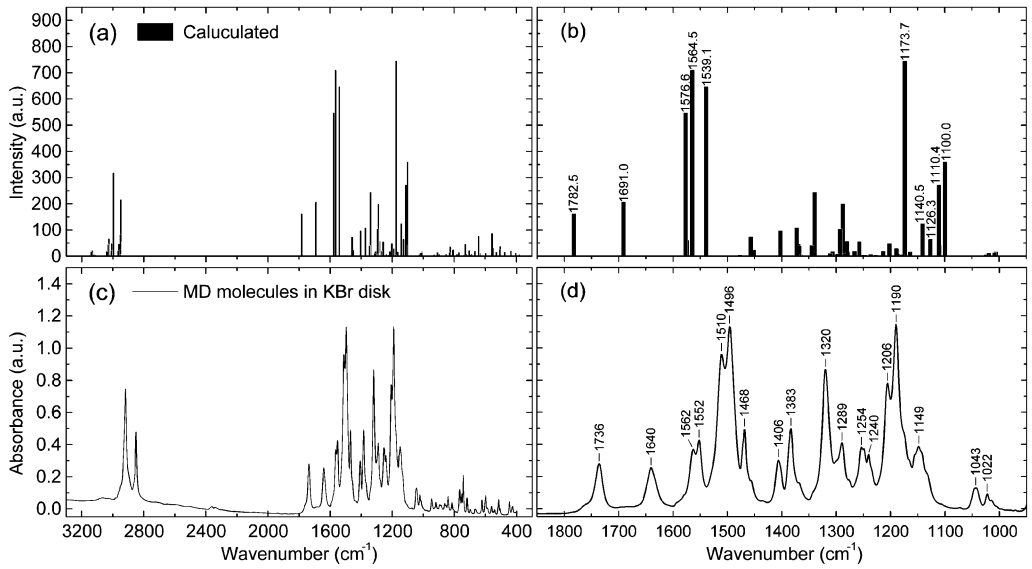

Figure 6. Comparison between calculated molecular vibrational modes and observed IR spectrum of MD molecules in the KBr disk. (a) and (b) indicate the calculated modes, and (c) and (d), the observed spectrum.

1.05:1:1.02:1.01, and the contrast of the lengths diminishes. This reflects the structure of $O^{\delta-}-C-C-C-C-C-N^{\delta+}$. In the case of the optimized structure, the ratio is 1.06:1:1.03:1.01, which indicates higher contrast than the structure of $O^{\delta-}-C-C-C-C-C-N^{\delta+}$ but lower than that of O═C−C═C−C═C−N. This result suggests that the resonant structure of the π-electron system of the dye backbone ($O{=}C-C{=}C-C{=}C-N \leftrightarrow O^{\delta-}-C-C-C-C-N^{\delta+}$) is well described by the optimized structure. It was reported that the dye, which has the backbone structure identical to that of the MD molecule, but with the butyl and ethyl substituents instead of the octadecyl and carboxymethyl substituents, respectively, has a dipole moment of 7.68 D.[35] This value also corresponds to the calculated value of 8.75 D for the MD molecule.

Ab Initio Calculation of Vibrational Modes. The calculated vibrational frequencies and relative intensities of the MD molecule in the optimized structure are schematically shown in Figure 6a together with the IR spectrum of the MD molecules in the KBr disk in Figure 6c. The overall feature of the calculated spectrum in Figure 6a reproduces the observed spectrum in Figure 6c quite well; the calculated two intense peaks around 3000 cm^{-1} correspond to the antisymmetric and symmetric CH_2 stretching modes observed at 2920 and 2850 cm^{-1}, respectively, and all calculated peaks below 2800 cm^{-1} reside in the 1800∼1000 cm^{-1} region, which again corresponds well to the result of observation. The calculated and observed spectra expanded in the 1800∼1000 cm^{-1} region are shown in Figure 6, parts b and d, respectively. The observed peak at 1738 cm^{-1}, which is mainly due to the C═O stretching mode of the carboxyl group, corresponds to the calculated one at 1782.5 cm^{-1}. The other nine vibrational modes are schematically shown in Figure 7 for calculated peaks with appreciable intensities in order to facilitate the assignments of main observed bands. From the figure, it is clear that the mode of the peak calculated at 1691.0 cm^{-1} is mainly due to the C═O stretching of the rhodanine ring, which corresponds to the observed peak at 1640 cm^{-1}. The modes for the peaks calculated at 1576.6, 1564.5, and 1539.1 cm^{-1} are the stretching modes of the central conjugated system coupled with a CH in-plane bending and a CC stretching mode of the phenyl ring of the benzothiazole group (see Figure 7). Presumably, these bands are ascribable to the strong doublet features at 1510 and 1496 cm^{-1} observed for MD molecules in the KBr disk and the broad band centered at 1485 cm^{-1} observed for the J-aggregate monolayers in Figure 2.

One of the marker bands for the phase transition observed near 1180 cm^{-1} (1188 cm^{-1} for the J-aggregate on subphase[100%] and 1177 cm^{-1} for the aggregate on subphase[0%], see Figure 2), which is the counterpart of the 1190 cm^{-1} band observed for MD molecules in the KBr disk, can be ascribed to the calculated peak at 1173.7 cm^{-1}, because of the good correspondence in frequency and intensity between the marker band and the result of the calculation in Figure 6b. Figure 7 indicates that this band is due to a mixed mode of a CH_2 twisting of the carboxymethyl group and the C═S stretching of the rhodanine ring. Figure 6b suggests that either the calculated peak at 1110.4 cm^{-1} or that at 1100.0 cm^{-1} corresponds to another marker band observed at 1146 cm^{-1} for the J-aggregate on subphase[100%] and 1126 cm^{-1} for the aggregate on subphase[0%]. As can be seen from Figure 7, the former band is due to a CH_2 wagging vibration of the carboxymethyl group of the rhodanine ring coupled with in-plane CH bending modes of the conjugated backbone and the benzothiazole group and the latter due to a coupled mode of CH_2 wagging and COH bending vibrations of the carboxyl group. The calculation was performed on the MD molecule with the protonated form of the carboxymethyl group of the rhodanine, whereas the group in the J-aggregate monolayer is in a dissociated form interacting with the counterion (Cd^{2+} or Mg^{2+}). Presumably, the dissociation affects largely the frequency and intensity of the calculated peak at 1100.0 cm^{-1}, because, as mentioned above, the COH bending mainly contributes to this peak. Then, it is impossible for this peak to be ascribed to the marker band. From this reasoning, we tentatively concluded that the calculated peak at 1110.4 cm^{-1} corresponds to the marker band. (The effect of the dissociation on the frequency and modes of the calculated peaks at 1173.7 and 1110.4 cm^{-1} is not so large to hamper the approximate assignments of these bands based on the calculated vibrational modes in Figure 7.) Thus, both of the marker bands are associated with the CH_2 vibrations of the carboxymethyl group mixed with the C═S stretching mode or the CH bending modes of the MD backbone and the benzothiazole group. It is reasonable to consider that the IR bands with these modes of the carboxymethyl group change their frequencies upon chang-

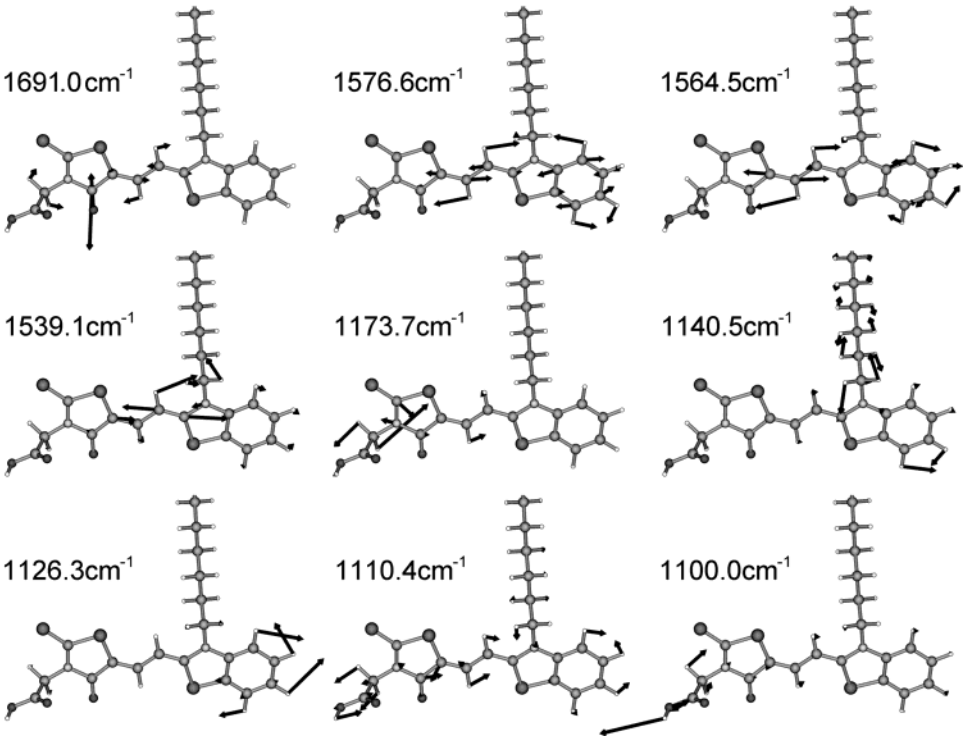

Figure 7. Schematic illustrations of the calculated vibrational modes locating at 1691.0, 1576.6, 1564.5, 1539.1, 1173.7, 1140.5, 1126.3, 1110.4, and 1100.0 cm^{-1}. The octadecyl chain of the MD molecule is omitted to be illustrated for simplicity.

ing the metal ions ($Mg^{2+} \leftrightarrow Cd^{2+}$) at the coordination site at the carboxylate group of the carboxymethyl group in the MD molecule, corroborating that the phase transition accompanies the exchange of the metal ions. (Figure 7 indicates that the calculated bands at 1140.5 and 1126.3 cm^{-1} are mainly due to a CH_2 twisting of the alkyl group coupled with CH in plane bending modes of the benzothiazole group and mainly due to a CH in plane bending mode of the benzothiazole group, respectively. It is hard to consider that the bands with these modes change their frequencies on changing the chelation metals with the carboxylate group.)

Conclusions

In situ observation of the J-aggregate phase transition at the air−water interface was performed by using the external infrared reflection absorption spectroscopy, indicating that the absorption bands at 1177 and 1126 cm^{-1} observed for the LT phase shift to those at 1188 and 1146 cm^{-1} for the HT phase; the reversible change of the band positions takes place during the transition, just as the positions of the J-band change reversibly between 620 nm (the LT phase) and 595 nm (the HT phase). The marker bands for the LT phase (1177 and 1126 cm^{-1}) were observed for the J-aggregate monolayer on the aqueous subphase containing only Mg^{2+} (subphase[0%]) exhibiting the J-band at 620 nm, whereas the marker bands for the HT phase (1188 and 1146 cm^{-1}) were observed for the monolayer on the aqueous subphase containing only Cd^{2+} (subphase[100%]) exhibiting the J-band at 595 nm. These results suggest that the phase transition from the LT phase to the HT phase accompanies the exchange of the metal ions interacting with the MD molecule from Mg^{2+} to Cd^{2+}.

The molecular structure of the MD molecule obtained by the ab initio calculation based on DFT corresponded appreciably well to the experimental result obtained by X-ray diffraction analysis of the J-aggregate crystal.[34] The ab initio vibrational calculation performed on the optimized structure of the MD molecule indicated that the marker bands are mainly associated with the CH_2 vibrations of the carboxylate group of the rhodanine group, where the carboxylate group forms the coordination site of the counterions. Thus, the ab initio calculation corroborates the conclusion that the phase transition takes place accompanying the exchange of the chelating metal ions. The exchange affects the degree of the conjugation of the dye backbone and/or the molecular packing structure of the J-aggregate,[23] which are main reasons for the shift of the J-band[1] due to the phase transition.

Acknowledgment. We thank Dr. Y. Urai (Waseda University) for the helpful instruction of the external IR reflection absorption measurements and are grateful to Dr. C. Ohe (Waseda University) for the fruitful discussions on the ab initio calculations. N.K. acknowledges the JSPS for a Young Scientists Research Fellowship. Financial supports for this work was provided by the Ministry of Education, Culture, Sports, Science and Technology, Grant-in-Aid for Encouragement of Young Scientist, 13750019, 2001, and Waseda University Grant for Special Research Projects (Individual Research, 2001A-111).

References and Notes

(1) (a) Kuhn, H.; Möbius, D. In *Physical Methods of Chemistry*, 2nd ed.; Rossiter, B. W., Baetzold, R. C., Eds.; John Wiley & Sons: New York, 1993; Chapter 6. (b) Kobayashi, T., Ed. *J-Aggregates*; World Scientific: Singapore, 1996.

(2) Harz, A. H. *Photogr. Sci. Eng.* **1974**, *18*, 323.

(3) Sayama, K.; Tsukagoshi, S.; Hara, K.; Ohga, Y.; Shinpou, A.; Abe, Y.; Suga, S.; Arakawa, H. *J. Phys. Chem. B* **2002**, *106*, 1363.

(4) (a) Furuki, M.; Tian, M.; Sato, Y.; Pu, L. S.; Tatsuura, S.; Wada, O. *Appl. Phys. Lett.* **2000**, *77*, 472. (b) Tatsuura, S.; Wada, O.; Furuki, M.; Tian, M.; Sato, Y.; Iwasa, I.; Pu, L. S. *Opt. Quantum Electron.* **2001**, *33*, 1089.

(5) Jelly, E. E. *Nature* **1936**, *138*, 1009.

(6) Scheibe, G. *Angew. Chem.* **1936**, *49*, 563.

(7) (a) Stuganova, I. *J. Phys. Chem. A* **2000**, *104*, 9670. (b) Zweck, J.; Penzkofer, A. *Chem. Phys.* **2001**, *269*, 399. (c) von Berlepsch, H.; Böttcher, C. *J. Phys. Chem. B* **2002**, *106*, 3146.

(8) García-Jiménez, F.; Khramov, M. I.; Sánchez-Obregón, R.; Collera, O. *Chem. Phys. Lett.* **2000**, *331*, 42.

(9) (a) Furuki, M.; Wada, O.; Pu, L. S.; Sato, Y.; Kawashima, H.; Yani, T. *J. Phys. Chem. B* **1999**, *103*, 7607. (b) Owens, R. W.; Smith, D. A. *Langmuir* **2000**, *16*, 562. (c) Ono, S. S.; Yamamoto, S.; Yao, H.; Matsuoka, O.; Kitamura, N. *Appl. Surf. Sci.* **2001**, *177*, 189. (d) Ikegami, K. *Jpn. J. Appl. Phys.* **2002**, *41*, 5444.

(10) (a) Hirano, Y.; Okada, T. M.; Miura, Y. F.; Sugi, M.; Ishii, T. *J. Appl. Phys.* **2000**, *88*, 5194. (b) Nakajima, H.; Kometani, N.; Asami, K.; Yonezawa, Y. *J. Photochem. Photobiol. A: Chem.* **2001**, *143*, 161. (c) Hamanaka, Y.; Kurasawa, H.; Nakamura, A.; Uchiyama, Y.; Marumoto, K.; Kuroda, S. *Chem. Phys. Lett.* **2002**, *363*, 233.

(11) (a) Fukutake, N.; Takasaka, S.; Kobayashi, T. *Chem. Phys. Lett.* **2002**, *361*, 42. (b) Vacha, M.; Takei, S.; Hashizume, K.; Sakakibara, Y.; Tani, T. *Chem. Phys. Lett.* **2000**, *331*, 387. (c) Scheblykin, I. G.; Bataiev, M. M.; Van der Auweraer, M.; Vitukhnovsky, A. G. *Chem. Phys. Lett.* **2000**, *316*, 37. (d) Zhou, H. S.; Watanabe, T.; Mito, A.; Asai, K.; Ishigure, K.; Honma, I. *J. Sol-Gel Sci. Technol.* **2000**, *19*, 803.

(12) (a) Kometani, N.; Tsubonishi, M.; Fujita, T.; Asami, K.; Yonezawa, Y. *Langmuir* **2001**, *17*, 578. (b) Hranisavljevic, J.; Dimitrijevic, N. M.; Wurtz, G. A.; Wiederrecht, G. P. *J. Am. Chem. Soc.* **2002**, *124*, 4537. (c) Lu, L.; Jones, R. M.; McBranch, D.; Whitten, D. *Langmuir* **2002**, *18*, 7706.

(13) Dai, Z.; Dähne, L.; Donath, E.; Möhwald, H. *J. Phys. Chem. B* **2002**, *106*, 11501.

(14) Garoff, R. A.; Litzinger, E. A.; Connor, R. E.; Fishman, I.; Armitage, B. A. *Langmuir* **2002**, *18*, 6330.

(15) (a) Sugi, M.; Saito, M.; Fukui, T.; Iizima, S. *Thin Solid Films* **1985**, *129*, 15. (b) Kawaguchi, T.; Iwata, K. *Thin Solid Films* **1990**, *191*, 173.

(16) (a) Ando, E.; Miyazaki, J.; Morimoto, K.; Nakahara, H.; Fukuda, K. *Thin Solid Films* **1985**, *133*, 21. (b) Unima, Y.; Miyata, A. *Thin Solid Films* **1989**, *179*, 497. (c) Matsumoto, M.; Nakazawa, T.; Azumi, R.; Tachibana, H.; Yamanaka, Y.; Sakai, H.; Abe, M. *J. Phys. Chem. B* **2002**, *106*, 1148.

(17) Shklyarevskiy, I. O.; Boamfa, M. I.; Christianen, P. C. M.; Touhari, F.; van Kempen, H.; Deroover, G.; Callant, P.; Maan, J. C. *J. Chem. Phys.* **2002**, *116*, 8407.

(18) Kato, N.; Saito, K.; Uesu, Y. *Chem. Phys. Lett.* **2000**, *326*, 395.

(19) Kato, N.; Saito, K.; Serata, K.; Aida, H.; Uesu, Y. *J. Chem. Phys.* **2001**, *115*, 1473.

(20) (a) Kato, N.; Aida, H.; Uesu, Y. *J. Korean Phys. Soc.* **1998**, *32*, S1076. (b) Iriyama, K.; Yoshiura, M.; Ozaki, Y.; Ishii, T.; Yausi, S. *Thin Solid Films* **1985**, *132*, 229.

(21) Gains, G. L., Jr. *Insoluble Monolayers at Liquid−gas Interfaces*; Wiley-Interscience: New York, 1966; Chapter 2, p 156.

(22) (a) Kato, N.; Saito, K.; Uesu, Y. *Nonlinear Opt.* **2000**, *25*, 171. (b) Kato, N.; Saito, K.; Uesu, Y. *Colloids Surf. A: Physicochem. Eng. Aspects* **2002**, *198*, 173.

(23) (a) Kato, N.; Shin, Y.; Uesu, Y. *Mater. Res. Soc. Symp. Proc.* **2001**, *660*, JJ5.33.1. (b) Kato, N.; Shin, Y.; Uesu, Y. *Ferroelectrics* **2002**, *269*, 285. (c) Kato, N.; Hirosawa, I.; Sato, M.; Ikeda, N.; Uesu, Y. *Ferroelectrics* **2003**, *286*, 921.

(24) Tani, T.; Kikuchi, S. *Bull. Soc. Sci. Photo. Jpn.* **1968**, *18*, 1.

(25) (a) Fujimoto, Y.; Ozaki, Y.; Takayanagi, M.; Nakata, M.; Iriyama, K. *J. Chem. Soc., Faraday Trans.* **1996**, *92*, 413. (b) Fujimoto, Y.; Ozaki, Y.; Iriyama, K. *J. Chem. Soc., Faraday Trans.* **1996**, *92*, 419.

(26) (a) Takayanagi, M.; Nakata, M.; Ozaki, Y.; Iriyama, K.; Tasumi, M. *J. Mol. Struct.* **1997**, *405*, 239. (b) Takayanagi, M.; Nakata, M.; Ozaki, Y.; Iriyama, K.; Tasumi, M. *J. Mol. Struct.* **1997**, *407*, 85.

(27) Ikegami, K.; Mingotaud, C.; Lan, M. *J. Phys. Chem. B* **1999**, *103*, 11261.

(28) Lan, M.; Ikegami, K. *Thin Solid Films* **2001**, *384*, 120.

(29) Ikegami, K.; Mingotaud, C.; Lan, M. *Thin Solid Films* **2001**, *393*, 193.

(30) Mendelsohn, R.; Brauner, J. W.; Gericke, A. *Annu. Rev. Phys. Chem.* **1995**, *46*, 305.

(31) (a) Matsuura, H.; Yoshida, H. In *Handbook of Vibrational Spectroscopy*; Chalmers, J. M., Griffiths, P. R., Eds.; Wiley & Sons: New York, 2002; Vol. 3, p 4203. (b) Ohe, C.; Ando, H.; Sato, N.; Urai, Y.; Yamamoto, M.; Itoh, K. *J. Phys. Chem. B* **1999**, *103*, 435.

(32) Urai, Y.; Ohe, C.; Itoh, K.; Yoshida, M.; Iimura, K.; Kato, T. *Langmuir* **2000**, *16*, 3920.

(33) Frisch, M. J.; Trucks, G. W.; Schlegel, H. B.; Scuseria, G. E.; Robb, M. A.; Cheeseman, J. R.; Zakrzewski, V. G.; Montgomery, J. A., Jr.; Stratmann, R. E.; Burant, J. C.; Dapprich, S.; Millam, J. M.; Daniels, A. D.; Kudin, K. N.; Strain, M. C.; Farkas, O.; Tomasi, J.; Barone, V.; Cossi, M.; Cammi, R.; Mennucci, B.; Pomelli, C.; Adamo, C.; Clifford, S.; Ochterski, J.; Petersson, G. A.; Ayala, P. Y.; Cui, Q.; Morokuma, K.; Malick, D. K.; Rabuck, A. D.; Raghavachari, K.; Foresman, J. B.; Cioslowski, J.; Ortiz, J. V.; Stefanov, B. B.; Liu, G.; Liashenko, A.; Piskorz, P.; Komaromi, I.; Gomperts, R.; Martin, R. L.; Fox, D. J.; Keith, T.; Al-Laham, M. A.; Peng, C. Y.; Nanayakkara, A.; Gonzalez, C.; Challacombe, M.; Gill, P. M. W.; Johnson, B. G.; Chen, W.; Wong, M. W.; Andres, J. L.; Head-Gordon, M.; Replogle, E. S.; Pople, J. A. *Gaussian 98*, revision A.11.2; Gaussian, Inc.: Pittsburgh, PA, 2001.

(34) Nüesch, F.; Grätzel, M.; Nesper, R.; Shklover, V. *Acta Crystallogr.* **1996**, *B52*, 277.

(35) Sturmer, D. M. In *Special Topics in Heterocyclic Chemistry*; Weissberger, A., Taylor, E. C., Eds.; John Wiley & Sons: New York, 1977; Chapter 8, p 477.